biomass

MDPI

Article

Investigation on the Potential and Suitability of Novel Plantain Peel Biomass for Energy Production

Osarue Osaruene Edosa [1,2], Francis Kunzi Tekweme [1] and Kapil Gupta [1,*]

[1] Department of Mechanical and Industrial Engineering Technology, University of Johannesburg, Johannesburg 2028, South Africa; oedosa@tubmanu.edu.lr (O.O.E.)
[2] Department of Mechanical Engineering, College of Engineering and Technology, William V.S. Tubman University, Harper P.O. Box 3570, Maryland County, Liberia
* Correspondence: kgupta@uj.ac.za

Abstract

Biomass, particularly agricultural waste, has emerged as a highly attractive alternative fuel source for domestic and industrial applications. This study investigates the suitability and potential of plantain peel biomass (PPB) as a viable feedstock for bioenergy production. The PPB was comprehensively characterized using proximate and ultimate analyses, thermogravimetric analysis (TGA), Fourier-transform infrared (FTIR) spectroscopy, and scanning electron microscopy coupled with energy-dispersive X-ray spectroscopy (SEM-EDS). Experimental results indicate that the weight ratio of plantain peel (skin) to unpeeled plantains ranges from 27% to 47%. Proximate analysis of the PPB yielded volatile matter (VM) of 65.8% and fixed carbon (FC) of 14.5%, suggesting substantial energy potential. The ultimate analysis results, conducted on a dry, ash-free basis, were used to determine the biomass higher heating value (HHV), which ranged from 13.93 to 16.35 MJ/kg. TGA showed that the thermal decomposition of PPB is typical of lignocellulosic biomass, occurring in three distinct stages over a temperature range of 25 to 1000 °C. FTIR spectroscopy identified O-H and C-H as key functional groups present in the PPB, further supporting its viability for biofuel production. Furthermore, SEM micrographs revealed a porous surface texture with heterogeneous particle sizes and shapes. At the same time, EDS confirmed carbon (C), potassium (K), and oxygen (O) as the dominant elements, alongside trace amounts of magnesium (Mg), silicon (Si), phosphorus (P), chlorine (Cl), and iron (Fe). In conclusion, PPB represents a promising and sustainable feedstock for biofuel production in both domestic and industrial sectors.

Keywords: biomass; fuel; pyrolysis; ash; TGA; SEM

Check for updates

Received: 4 July 2026
Revised: 26 August 2026
Accepted: 26 August 2026
Published: 1 September 2026

Copyright: © 2026 by the authors. Licensee MDPI, Basel, Switzerland. This article is an open access article distributed under the terms and conditions of the Creative Commons Attribution (CC BY) license.

1. Introduction

Biomass fuel is an important renewable and environmentally sustainable energy source widely used for domestic and industrial applications as a substitute for fossil fuels [1]. Biomass consists of organic materials derived from plants and animals, including wood, agricultural residues, garbage, animal dung, and sewage [2,3]. These materials can be converted into energy through direct combustion, thermochemical processes such as pyrolysis and gasification, and chemical or biological methods [4,5]. While combustion requires oxygen, pyrolysis occurs in an inert environment to prevent oxidation and enable the production of fuels such as biochar and briquettes [4,6]. The resulting energy products from biomass include biochar, ethanol, biodiesel, and biogas [1,7]. According to the United

States Energy Information Administration (EIA), biomass accounted for approximately 5% of the total primary energy consumed in the US in 2023, underscoring its growing relevance as a sustainable energy resource [8].

Agricultural biomass has attracted considerable attention due to its abundance and renewable nature. Its energy potential is largely influenced by its organic component, particularly the presence of cellulose, hemicellulose, and lignin [9]. Inorganic components, including ash-forming elements such as carbon, silicon, potassium, calcium, and sodium, further influence its suitability for composite fabrication [10]. For example, biomass with low ash content is generally more suitable for liquid biofuels, whereas higher FC content favors both liquid and solid fuel applications such as bioethanol, briquettes, and biochar [11,12]. Despite extensive studies on agricultural residues such as rice husk, corn cob, palm kernel shell, and groundnut shells, little to no research has been conducted on PPB as a potential energy source [7,12].

Plantain (*Musa paradisiaca*) is widely cultivated in tropical regions, particularly in West Africa, where it serves as a staple food crop. Major producers include Nigeria, Ecuador, Colombia, Ghana, and Cameroon. The peel, which constitutes approximately 27–47% of the fruit's total weight, is typically discarded during processing, contributing to increasing volumes of agricultural waste. With rising global demand for plantains and their derived products due to their nutritional value, plantain peel waste generation is expected to increase, posing potential environmental challenges if not properly managed.

Characterization is a fundamental requirement for assessing the suitability of biomass for bioenergy production. Understanding the physicochemical, structural, and thermal properties of biomass is essential because these characteristics influence the selection of appropriate pretreatment and conversion technologies, energy content, fuel quality, conversion efficiency, and environmental impact [1,5]. Furthermore, characterization data provide valuable information for estimating the calorific value of biomass, designing and optimizing energy-conversion systems, and managing emissions during thermochemical processes. For instance, the volatile matter and fixed carbon contents of biomass are key indicators of its energy potential. Similarly, the nature and distribution of functional groups within the biomass structure influence its chemical reactivity, thermal stability, and fuel suitability. Some of the characterization techniques and their functions include the following: proximate analysis evaluates MC, VM, FC, and ash, while ultimate analysis determines the elemental composition (C, H, O, N, and S) to estimate the heating (calorific) value. Additional methods such as TGA, FTIR, XRD, and SEM-EDS provide insights into thermal behavior, functional groups, crystallinity, and surface morphology, respectively [7,11,13].

Utilizing PPB for energy production contributes to several sustainable development goals (SDGs), such as mitigating greenhouse gases, developing the rural economy, and promoting sustainable waste management that aligns with the principles of reduce, reuse, and recycle [14,15]. Accordingly, this study investigates the potential of novel PPB as a renewable energy source. The PPB is novel because no PPBs sourced from Liberia and characterized for energy production have been reported in the literature. The PPB was characterized using proximate and ultimate analyses, TGA, FTIR, and SEM-EDS to evaluate its suitability for energy generation. This study aims to contribute to the development of sustainable biomass resources and expand the utilization of plantain peels.

2. Materials and Methods

2.1. PPB Preparation and Characterization

A substantial quantity of PPB sourced from Harper, Maryland County, Liberia, was thoroughly cleansed to remove dirt and other contaminants. The PPB was dried for weeks at ambient temperature to reduce the moisture content and subsequently stored in a polythene

bag for further use. The dried PPBs were pulverized and sieved to an average particle size of 70 microns before characterization. In no particular order, the characterization of the PPB included SEM-EDS, FTIR, TGA, and proximate and ultimate analyses. Figure 1a–f show unripe plantain, edible plantain, fresh plantain peels, dried plantain peels, plantain peel powder, and plantain peel ash.



Figure 1. (**a**) Unripe plantain, (**b**) edible plantain, (**c**) fresh plantain peels, (**d**) dried plantain peels, (**e**) dried plantain peel powder, (**f**) plantain peel ash.

2.2. Determination of the Weight Fraction of Plantain Peel

To accurately estimate the weight fraction of the PPB, some unripe and unpeeled plantains were purchased and cleaned, and each was weighed on a digital balance and recorded as P_1. Each unpeeled plantain was peeled, weighed, and recorded as P_2 for the edible plantain and P_3 for the peels, as shown in Table 1. The percentage weight of the plantain peel as a function of the total weight of the unpeeled plantain is determined using Equation (1).

$$PPwt(\%) = ({}^{P_3}/_{P_1}) \times 100 \quad (1)$$

2.3. Density of the PPB

To determine the density of the PPB powder and ash residue, a small fraction of the powder and ash residue was placed in a gas pycnometer (BetterPyc 380) Bettersize, Noi, Vietnam. The instrument measures the mass and volume of the PPB powder sample and then estimates the densities of the powder and ash residue. The pycnometer measures the density of solid powders with an accuracy of 0.01%.

Table 1. Experimental data for the weight fraction of plantain peel.

Weight of Plantain Before Peeling (P_1) (g)	Weight of Edible Plantain After Peeling (P_2) (g)	Weight of Plantain Peel (P_3) (g)
476	290	186
316	169	147
479	275	204
189	137	52
216	134	82
200	127	73

2.4. Proximate Analysis of the PPB

The proximate analysis of the PPB was performed to determine the percentage of MC, VM, ash content, and FC. The experimental procedure follows the ASTM D3172 standard [16]. Utilizing the conventional furnace method, the percentage of MC, VM, ash content, and FC of the PPB were determined.

2.4.1. Moisture Content (MC)

To determine the MC of the PPB, the mass of the crucible was first determined and recorded as (W_1). After that, the porcelain crucible was filled with the PPB powder sample, weighed, and recorded as (W_2). It was then placed in a tube furnace under a nitrogen atmosphere and heated to 100 ± 5 °C for 30 min. The furnace was switched off after 30 min of heating to cool to ambient temperature. The procedure was repeated to get an average mass of the residue, which was recorded as W_3. The percentage MC of the PPB was estimated by simple weight loss as expressed in Equation (2).

$$MC(\%) = \left({}^{W_2 - W_3}/_{W_2 - W_1}\right) \times 100 \quad (2)$$

The total solid mass (TSM %) can be estimated using Equation (3) or (4).

$$TSM(\%) = 100 - MC(\%) \quad (3)$$

$$TSM(g) = W_3 - W_1 \quad (4)$$

2.4.2. Volatile Matter (VM)

The crucible containing the dried PPB, recorded as W_3, was placed in the tube furnace and heated to a temperature of 950 ± 5 °C in a nitrogen atmosphere to determine the combustible matter. After soaking at this temperature for 1 h, the furnace was switched off and allowed to cool to room temperature. The procedure was repeated to get an average mass of the residue, which was recorded as W_4. The VM, which is the solid mass loss after PPB decomposition, was determined using Equation (5).

$$VM(\%) = \left({}^{W_3 - W_4}/_{W_3 - W_1}\right) \times 100 \quad (5)$$

2.4.3. Ash Content

To estimate the percentage of ash residue, the crucible and its contents, recorded as W_4, were placed in the furnace and heated to a temperature of 750 ± 5 °C in an oxygen atmosphere. After holding at this temperature for 1 h, the furnace was cooled to room temperature. The procedure was repeated to get an average mass of the ash residue, which was recorded as W_5. The percentage of the ash residue was estimated using Equation (6).

$$Ash(\%) = \left({}^{W_5 - W_1}/_{W_3 - W_1}\right) \times 100 \quad (6)$$

2.4.4. Fixed Carbon

The FC represents the non-volatile, combustible carbon and can be estimated using Equation (7). The data for the proximate analysis are presented in Table 2.

$$FC(\%) = 100 - (MC\% + VM\% + Ash\%) \quad (7)$$

Table 2. Experimental data for proximate analysis of PPB using the furnace method.

Parameters	Designation	Experimental Values (g)
Mass of crucible	W_1	8.378
Mass of crucible and PP powder @ room temperature	W_2	9.555
Mass of crucible and PP powder @ 100 ± 5 °C	W_3	9.443
Mass of crucible and PPB @ 950 ± 5 °C	W_4	8.697
Mass of crucible and PPB @ 750 ± 5 °C	W_5	8.510

2.5. TGA of PPB

The pyrolytic characteristic of the PPB was determined using a thermogravimetric analyzer, Universal V4.5A (SDT Q600 V20.9 Build 20), New Castle, DE, USA. Following the ASTM D5142 standard [16], 7.9 mg of the PPB powder was placed in the analyzer, where it was heated to a temperature range of 0 to 1000 °C at a heating rate of 20 °C/min under nitrogen gas with a flow rate of 35 mL/min to create an inert atmosphere in the heating chamber.

2.6. Ultimate Analysis of PPB

The percentage weight of hydrogen, sulfur, carbon, and nitrogen in the PPB was estimated using the ultimate analysis method, as specified in the ASTM D5373 standard [17]. Approximately 1.8 g of the PPB powder, on a dry ash-free basis, was placed in a TA instrument (Universal V4.5A, SDT Q600 V20.9 Build 20) and burned at an elevated temperature in a pure oxygen atmosphere. The weight percentages of C, H, N, and S were estimated using an elemental analyzer, while that of Oxygen (O) was calculated by weight difference, as expressed in Equation (8).

$$O\% = 100 - (C\% + H\% + N\% + S\%) \quad (8)$$

2.7. Heating (Calorific) Value of PPB

As reported in the literature, the HHV of biomass can be determined using either experimental or modeling methods [18,19]. The experimental method is seldom used due to the cost of the experimental setup as well as the close agreement between experimental and modeling results [20]. Several models have been developed to estimate the heating value of biomass. Some of these models are based on parameters from proximate or ultimate analyses [21–24]. The HHV of the PPB is determined using Equations (9)–(13) [23–27].

$$HHV = 0.3516(C) + 1.16225(H) - 0.1109(O) + 0.0628(N) + 0.10465(S) \quad (9)$$

$$HHV = 0.3137(C) + 0.7009(H) + 0.0318(O) - 1.3675 \quad (10)$$

$$HHV = 0.3491(C) + 1.1783(H) - 0.1034(O) - 0.0151(N) + 0.1005(S) - 0.0211(ash) \quad (11)$$

$$HHV = 0.3443(C) + 1.192(H) - 0.113(O) - 0.024(N) + 0.093(S) \quad (12)$$

$$HHV = 0.341(C) + 1.323(H) - 0.1194(O) - 0.1194(N) + 0.0685(S) - 0.0153(ash) \quad (13)$$

2.8. FTIR Analysis

To determine the various functional groups present in the PPB, an FTIR instrument (Perkin Elmer Spectrum Version 10.03.02, Shelton, CT, USA) was used. A small quantity of the PPB powder sample was mixed with KBr and placed in the instrument for examination. Scanning of the PPB sample was performed over the wavelength range of 400 to 4000 cm^{-1} to identify the various functional groups. A similar procedure was reported by previous studies [16,28].

2.9. SEM-EDS Analysis of PPB

The surface morphology and chemical composition of the PPB dry powder and ash residue were determined using SEM-EDS (JEOL JSM-6390, JEOL, Peabody, MA, USA). Before the examination, the PPB samples were coated with carbon to make them conductive.

3. Results and Discussion

3.1. The Density and Weight Fraction of PPB

The plantain peel is central to this study because of its potential for bioenergy production. As a veritable source of energy, it is important to estimate the weight of the peel (skin) as a ratio of the total weight of the unpeeled plantain to determine the amount of peel that can be generated per ton, with a view to estimating the amount of energy that can be harvested from the peels. Using Equation (1), the weight of the plantain peel, as a fraction of the total weight of the unpeeled plantain, is estimated to be 27–47%. It was observed that the larger the plantain, the larger the peel, and vice versa. The density of the plantain peel powder and ash was 2.34 g/cm^3.

3.2. Proximate Analysis Results of PPB

The proximate analysis of PPB is essential for evaluating its suitability for energy production [29]. The results of the proximate analysis are presented in Table 3. The findings indicate that the measured parameters fall within acceptable ranges when compared with previous studies [17,30,31]. The moisture content of biomass depends on the type of biomass and the drying methods (air- or oven-dried). A high MC is undesirable because it reduces the combustible fraction and overall energy value of the biomass. In addition, a high MC requires more energy to remove water and volatile gases before ignition can occur. Therefore, a low MC is preferable [29].

The volatile matter (VM) content of 65.8% indicates significant energy potential. This suggests that the combustible volatile component in the PPB is sufficient to support rapid ignition, flame propagation, and substantial energy release. However, excessively high VM values (e.g., greater than 90%) may result in excessive volatility, leading to incomplete combustion, increased emissions, and reduced heating value. Furthermore, a very high VM content decreases the proportion of FC in the biomass. Comparatively, the VM in PPB is higher than that of empty fruit branch (EFB) [13], tobacco stem [32], and lemongrass [33], but lower than that of melon seed shell [15], corn cob [16], and sweet sorghum stalk (SSS) [31].

FC represents the non-volatile combustible carbon, which directly influences the heating value of biomass. A relatively high FC content (e.g., approximately $\geq 10\%$) is desirable because it enhances fuel quality by supporting prolonged and sustained combustion [34]. Fixed carbon also contributes to char formation, which is an essential requirement for briquette production. It can be inferred that as FC content increases, VM content decreases, and vice versa [35].

Ash represents the non-combustible inorganic residue remaining after combustion. For efficient and clean combustion, a low ash content is generally preferred. High ash

content is generally undesirable because it increases solid residue generation, lowers the calorific value of biomass, and promotes slagging and fouling in thermochemical conversion systems, particularly gasification equipment. However, slagging can be minimized by maintaining the operating temperature below 900 °C [36].

Variations in ash content are influenced by several factors, including biomass type, plant species, combustion efficiency, geographical location, and soil characteristics. Woody biomass typically contains lower ash levels than herbaceous and agricultural biomass, whereas industrial biomass generally produces the highest ash content. Previous studies reported that the ash content of agricultural biomass can reach up to 20% [37,38]. Similarly, Marrugo et al. [16] reported an ash content of 24.71% for banana rachis, while Olupot et al. [39] reported ash contents ranging from 15.87% to 25.56% for different varieties of rice husks in Uganda. A practical approach to improving the fuel quality of high-ash biomass is to blend it with low-ash feedstocks, such as sawdust. This strategy reduces the overall ash content, improves combustion performance, and mitigates operational problems associated with ash deposition and slagging. Nevertheless, high ash content can be advantageous for composite reinforcement applications. Studies reported improvements in the properties of metal matrix composites (MMCs) through the incorporation of biomass ash [40,41].

Furthermore, the physicochemical properties of agricultural biomass vary considerably among plant species and even within the same biomass type. These variations are influenced by several factors, including geographical location, plant species, climatic conditions, soil characteristics, and cultivation practices [14,30]. For example, the physicochemical properties of plantain peel biomass from Nigeria, as reported by Williams et al. [42], differ from those of biomass from Liberia, as characterized in the present study. Similarly, Marrugo et al. [16] reported volatile matter and ash contents for palm kernel shell that differ from those reported by Onokwai et al. [7]. Likewise, the volatile matter content of lemongrass reported by Yahya et al. [35] differs from that reported by Madhu et al. [33]. These variations demonstrate the influence of feedstock origin and environmental conditions on biomass properties and highlight the importance of region-specific characterization. Consequently, the physicochemical data on PPB reported in this study provide novel information supporting its evaluation as a potential feedstock for bioenergy applications.

Table 3. Results of proximate analysis, ultimate analysis, and HHV of agricultural biomass.

Biomass Samples	MC (wt%)	VM (wt %)	Ash (wt%)	FC (wt %)	N (wt%)	C (wt%)	H (wt%)	S (wt%)	O (wt%)	HHV (MJ/Kg)	References
PPB	9.5	65.8	10.2	14.5	1.34	39.14	5.35	1.12	53.05	13.93–16.35	This work
MP	10.6	70.0	5.8	13.6	0.23	46.94	5.79	0.30	46.74	18.28	[43]
PA Wood	3.13	71.43	3.86	21.58	0.52	49.23	6.13	0.15	43.97	17.75	[44]
Palm kernel shell	0.40	73.70	3.50	22.40	0.12	48.28	5.39	0.03	46.18	21.65	[7]
Coconut shell	9.66	71.92	0.67	17.75	0.19	47.29	4.91	0.37	47.24	17.43	[10]
Melon seed shell	6.38	80.43	7.27	9.92	1.86	71.49	9.63	0.1	16.92	18.30	[15]
Lemon grass	8.02	59.99	8.02	24.78	1.54	39.34	5.81	0.01	53.30	17.20	[33]
Empty fruit bunch (EFB)	25.0	58.7	2.2	14.1	0.68	45.90	5.90	0.09	44.20	19.30	[13]
Peanut shell	5.16	80.24	6.12	8.48	1.03	46.86	6.84	0.29	44.98	18.64	[45]
Mixed Wood Sawdust (MWS)	8.82	73.34	6.59	11.25	1.32	46.66	6.60	0.64	44.78	16.23	[46]

3.3. Ultimate Analysis and Heating Value of PPB

The ultimate analysis of the PPB was conducted to determine the percentage weight fractions of hydrogen, sulfur, carbon, oxygen, and nitrogen required for determining its HHV. The HHV is one of the most important characteristics of biomass because it indicates the total amount of heat energy that can be generated during combustion [13]. The results of the ultimate analysis and HHV of the PPB are presented in Table 3. Carbon (C) and hydrogen (H) are the primary energy-contributing elements in biomass; therefore, an increase in their weight fractions generally increases the heating value [47]. In contrast,

elevated oxygen and nitrogen contents lower the energy density by reducing the heating value of biomass. Using commonly used Equations (9)–(13) reported in the literature and acceptable for HHV determination, the HHV of the PPB was calculated to be 14.30, 16.35, 14.56, 13.93, and 14.01 MJ/kg, respectively. This finding shows that the energy value of the PPB falls within the range of selected rice husk varieties from Uganda, as reported in [39], and mixed wood sawdust (MWS), as reported in [46]. However, this energy value is lower than that of matoke peel (MP) [43], palm kernel shell [7], Tectona grandis seeds (TGs) [47], and peanut shell [45]. As reported, these variations may be attributed to the combustion efficiency, biomass types, origin, and environmental and soil conditions.

Furthermore, the sulfur content of the PPB is relatively high compared with other biomass presented in Table 3. High sulfur content in biomass fuel can adversely affect fuel quality, contribute to air pollution through sulfur dioxide (SO_2) emissions, and accelerate engine corrosion.

3.4. TGA-DSC and TGA-DTG of PPB

The TGA–DSC and TGA–DTG of PPB, presented in Figure 2a,b, demonstrate that the pyrolytic decomposition of the biomass occurred in three distinct stages up to 1000 °C, consistent with the behavior of other lignocellulosic biomasses. The first stage, which occurred between 50 and 200 °C, involved the removal of moisture and volatile gases, resulting in a weight loss of approximately 8.7%, as illustrated in Figure 2a. This relatively low moisture content suggests reduced energy demand during drying and minimizes poor ignition problems [43].

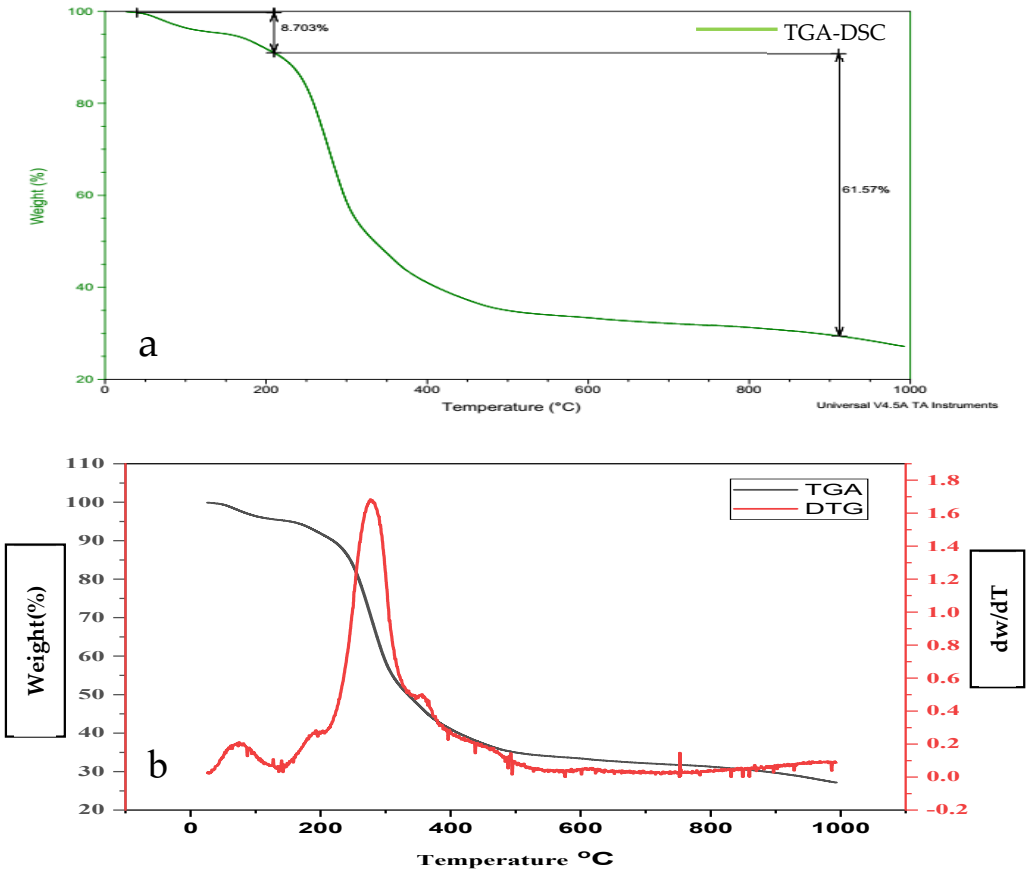


Figure 2. (**a**) TGA-DSC and (**b**) TGA-DTG graphs of PPB under nitrogen atmosphere.

The second stage corresponds to the active pyrolysis of the dried PPB and accounted for approximately 61.57% mass loss. As shown in Figure 2, decomposition occurred in

sequential stages associated with hemicellulose (200–300 °C), cellulose (300–450 °C), and lignin (450–650 °C) degradation [34,48]. Hemicellulose degradation is gradual due to its more amorphous structure and is represented by the small peak or shoulder in the DTG curve shown in Figure 2b. Cellulose decomposes rapidly within narrow temperature ranges because of its less complex and more volatile structures, leading to substantial mass loss. The largest peak in the DTG curve corresponds to T_{max}, and it indicates the temperature (~300 °C) at which the maximum mass loss occurred. In contrast, lignin decomposes gradually with a gradual mass loss over a broader temperature range because of its dense structure and high molecular weight [4,49].

The third stage is an extension of the second stage, and it shows the continuation of slow lignin degradation and char formation. The relatively flat section of the TGA curve during lignin degradation and char formation indicates gradual decomposition (mass loss) of carbonaceous structures despite increasing temperature. The resulting residue is rich in carbon [4,49,50].

Following pyrolysis in a nitrogen atmosphere, the remaining residue, composed mainly of fixed carbon and ash, accounted for approximately 29.73% of the original PPB mass. FC contributes to prolonged combustion and increases the HHV of PPB. Furthermore, the residual mixed FC and ash can undergo oxidation, releasing additional thermal energy and producing ash residue. The resulting ash, consisting primarily of metal and non-metal oxides, may also serve as an inorganic filler or reinforcement material in composite fabrication.

3.5. FTIR Analysis of PPB

FTIR spectroscopy, shown in Figure 3, was utilized to identify the functional groups and chemical compounds present in the PPB [51]. In an FTIR spectrum, higher wavenumbers correspond to higher energy levels and vice versa. When the spectrum is plotted as transmittance (as shown on the Y-axis of Figure 3), characteristic molecular absorptions appear as downward valleys. Conversely, these spectral features can be represented as upward peaks if an absorbance spectrum is used instead.

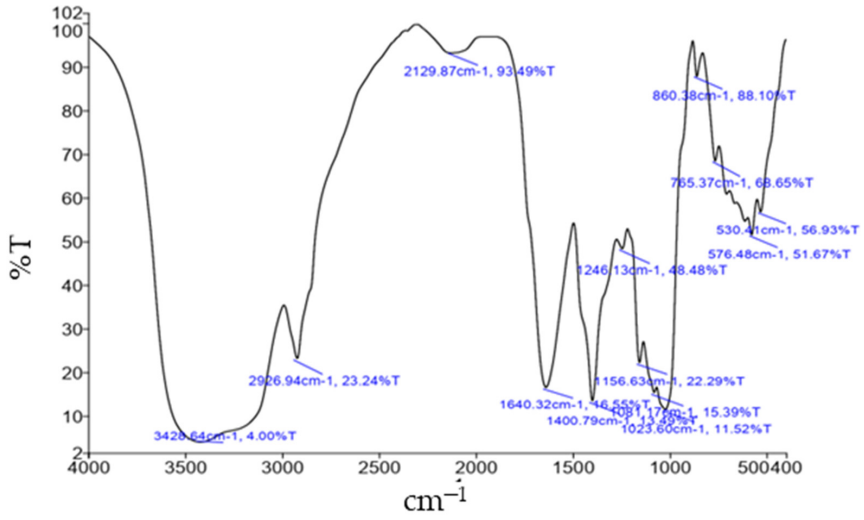


Figure 3. FTIR graph of PPB.

To systematically identify the various functional groups, the FTIR spectra can be categorized into four distinct regions based on their characteristic molecular vibrations [52]. These regions include a single bond (4000–2500 cm^{-1}), a triple bond (2500–2000 cm^{-1}), a double bond (2000–1500 cm^{-1}), and a fingerprint region (1500–500 cm^{-1}).

Table 4 outlines the specific functional groups and chemical compounds identified in the PPB, derived using a standard infrared spectroscopy correlation table. The detection of O-H stretching vibrations suggests the presence of hydrated compounds within the biomass. Specifically, the O-H group suggests the presence of bound water molecules or alcohols such as ethanol, methanol, and isopropanol.

Table 4. FTIR spectroscopy and the corresponding functional groups present in the PPB.

S/No	Wavenumber (cm^{-1})	Functional Group(s)	Chemical Compound
1	3428	O-H	Alcohol, phenol
2	2926	C-H	hydrocarbons
3	2129	C≡C	Alkyne
4	1640	C=C	Alkene/Aromatic
5	1400	C-H	Aliphatic, aromatic
6	1246	C-O-C	Ether/Carbohydrate
7	1156	C-O	Carbohydrate
8	1081	C-O	Carbohydrate
9	1023	C-O	Ether
10	860	C-H	Aromatics
11	765	C-H	Aromatics
12	576	C-Br, C-I	Bromide, Iodide
13	530	C-Br, C-I	Bromide, Iodide

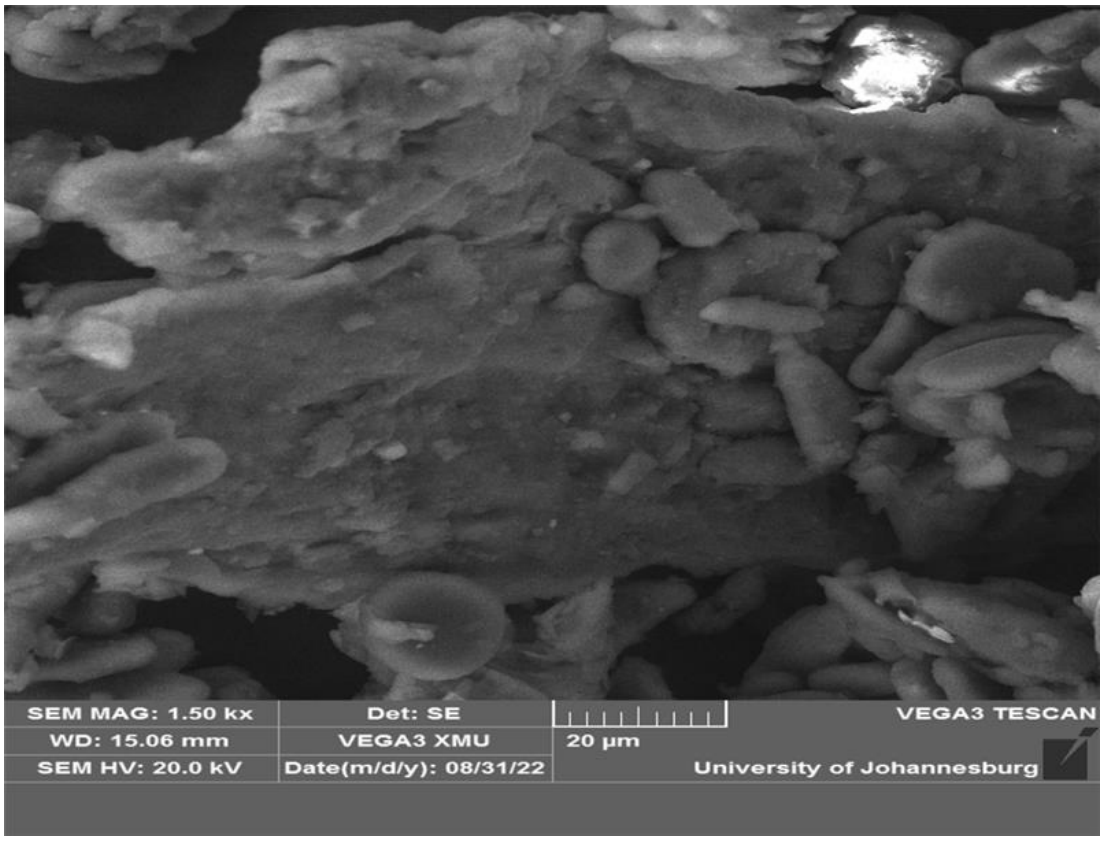
The C-H groups indicate hydrocarbon structures, which form the basic units of alkanes, alkenes, and alkynes. The concentration of C-H groups in plant matter directly influences its heating value, thereby affecting its efficiency as a biomass energy source. The C-O groups coexist with hydroxyl (O-H) groups to form the structural frameworks of hemicellulose, cellulose, and lignin, which indicate biofuel potential. They also suggest the presence of hydrated and oxygenated compounds. Identifying these functional groups in the PPB influences the choice for pretreatment and conversion pathways for biofuel production.

Finally, halo-compounds such as C-F, C-Cl, C-Br, and C-I are primarily concentrated within the fingerprint region, where they contribute to important ecological and biochemical functions.

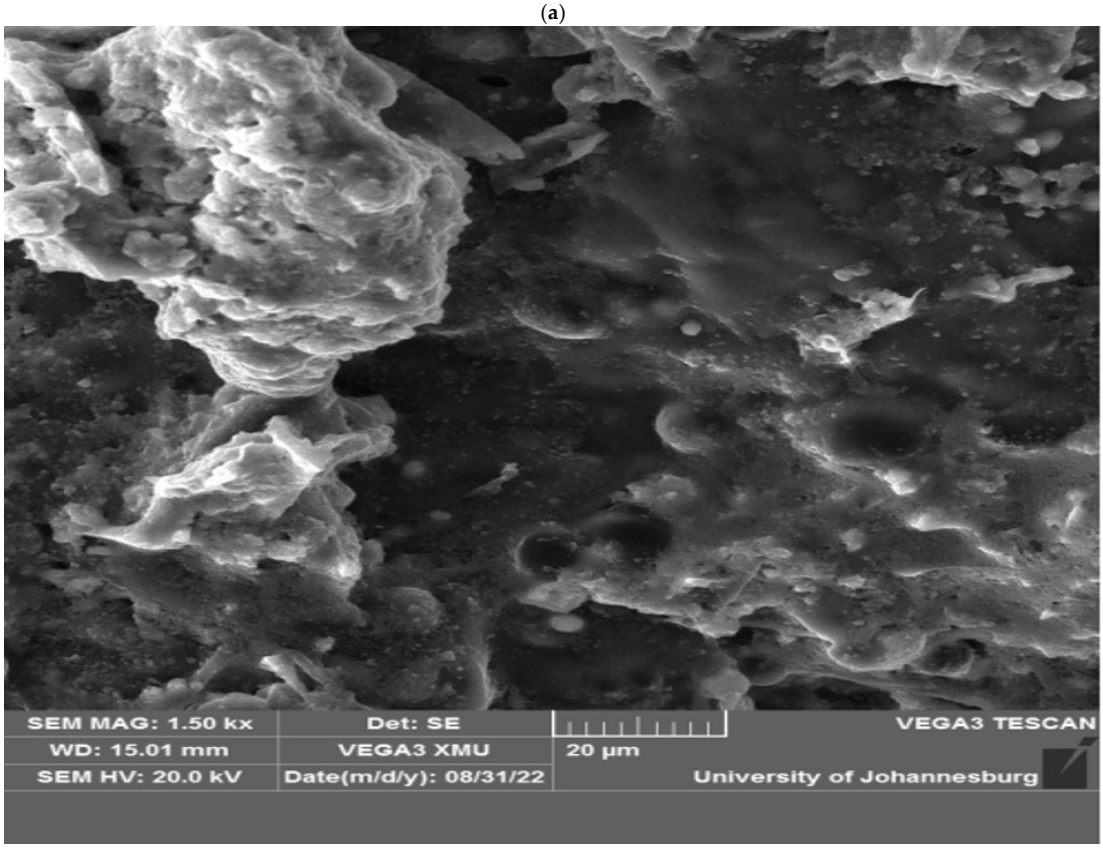
3.6. SEM-EDS Analysis Results of PPB

The SEM-EDS analysis of PPB provides valuable information on its physical, structural, and chemical characteristics, which are essential for optimizing biomass utilization and improving biofuel quality. The SEM micrograph presented in Figure 4 shows that the PPB powder consists of a heterogeneous distribution of particle sizes and morphologies, including oval, flaky, and irregular-shaped particles with porous surface textures. These porous structures are advantageous because they enhance catalyst penetration during thermochemical and biochemical conversion processes, thereby improving biomass conversion efficiency for biofuel production. The EDS analysis indicates the presence of carbon (C), potassium (K), oxygen (O), magnesium (Mg), silicon (Si), phosphorus (P), chlorine (Cl), and iron (Fe) in the PPB, as presented in Table 5. As observed from the table, apart from oxygen, carbon has the highest weight percentage. This may be attributed to the coating of the biomass powder during EDS analysis using carbon [53,54]. In addition, EDS is an effective technique for identifying inorganic elements that may contaminate biofuels or contribute to slagging and fouling during combustion. For instance, studies show that the presence of Na, K, S, and Cl in ash residue in the form of chlorides and sulfates in substantial amounts causes slagging in combustion equipment. Detecting these elements enables appropriate

pretreatment strategies to eliminate them, thereby minimizing operational challenges and improving fuel quality [55–58].



(**a**)



(**b**)

Figure 4. (**a**,**b**) SEM micrograph of plantain peel biomass.

Table 5. Elemental composition of PPB.

Elemental Composition (wt%)	C	Mg	Al	Si	P	S	Cl	K	O	Fe	N
Plantain peel powder	23.71	0.07	0.03	0.13	0.25	0.16	0.94	6.88	67.05	0.22	0.57

3.7. Advantages and Limitations of This Study

This study is significant because it addresses two major challenges: agricultural waste management and the need for sustainable energy resources. Firstly, it promotes the principles of reduce, reuse, and recycle by valorizing agricultural waste, thereby supporting the transition toward a circular economy and mitigating environmental pollution associated with improper waste disposal. Secondly, it investigates the potential of PPB as a feedstock for renewable energy production, which could help diversify energy resources and reduce the risk of fuel supply shortages. The characterization and pyrolysis of PPB provide important information on its physicochemical and thermal properties, thereby establishing a scientific basis for assessing its energy potential and identifying appropriate thermochemical conversion pathways. However, this investigation is subject to several limitations, including the lack of fully equipped laboratory facilities for comprehensive biomass characterization, pretreatment, and conversion into final energy products. Furthermore, the costs associated with biomass collection, transportation, processing, characterization, pretreatment, and subsequent conversion into bioenergy products represent significant challenges.

4. Conclusions

The key findings are summarized as follows:

i. Consumption of plantains generates substantial quantities of PPB. Without proper management through recovery, recycling, and reuse, the accumulation of PPB may contribute to environmental pollution.
ii. The proximate and thermogravimetric analyses showed that the total combustible component of PPB (%VM + %FC) is approximately 80%, indicating its significant potential for energy production.
iii. The presence of O–H and C–H bonds in PPB further supports its suitability as a biofuel feedstock. The O–H functional group suggests the presence of hydrated compounds, while the C–H bond, characteristic of hydrocarbons, contributes to the heating value of biomass and enhances its potential as an energy source.
iv. SEM showed that PPB powder and ash particles exhibit diverse morphologies, including oval, flaky, and irregular shapes, along with a porous surface texture. These characteristics may influence particle flowability and packing factor.

Recommendation for future work

Future studies should focus on the conversion of PPB into biofuels and solid bioenergy products, such as bioethanol and briquettes.

Author Contributions: Conceptualization, O.O.E., F.K.T. and K.G.; methodology, O.O.E., F.K.T. and K.G.; software, O.O.E.; validation, O.O.E.; formal analysis, O.O.E., F.K.T. and K.G.; investigation, O.O.E.; resources, F.K.T. and K.G.; data curation, O.O.E.; writing—original draft preparation, O.O.E.; writing—review and editing, F.K.T. and K.G.; visualization, O.O.E., F.K.T. and K.G.; supervision, F.K.T. and K.G.; project administration, F.K.T. and K.G.; funding acquisition, F.K.T. and K.G. All authors have read and agreed to the published version of the manuscript.

Funding: This research received no external funding.

Data Availability Statement: The raw data supporting the conclusions of this article will be made available by the authors on request.

Acknowledgments: The authors acknowledge the lab staff and facilities of the University of Johannesburg. Authors also acknowledge the use of Grammarly, free edition and ChatGPT—5.6 Luna model, free edition, for language editing of the entire manuscript.

Conflicts of Interest: The authors declare no conflicts of interest.

References

1. Verma, B.B.; Patle, S.D.; Dewangan, S.K. Recent advances and comparative insights of synthesis and characterization methods of solid biofuels derived from biomass waste. *Biomass Bioenergy* **2025**, *209*, 108980. [CrossRef]
2. Anvari, S.; Aguado, R.; Jurado, F.; Fendri, M.; Zaier, H.; Larbi, A.; Vera, D. Analysis of agricultural waste/byproduct biomass potential for bioenergy: The case of Tunisia. *Energy Sustain. Dev.* **2023**, *78*, 101367. [CrossRef]
3. Trivedi, K.; Sharma, A.; Kanabar, B.K.; Arunachalam, K.D.; Gautam, S. Comparative Analysis of Coal and Biomass for Sustainable Energy Production: Elemental Composition, Combustion Behavior and Co-Firing Potential. *Water Air Soil Pollut.* **2024**, *235*, 698. [CrossRef]
4. Kumar, A.; Wang, L.; Dzenis, Y.A.; Jones, D.D.; Hanna, M.A. Thermogravimetric characterization of corn stover as gasification and pyrolysis feedstock. *Biomass Bioenergy* **2008**, *32*, 460–467. [CrossRef]
5. Vilas-Boas, A.C.M.; Tarelho, L.; Moura, J.; Gomes, H.; Marques, C.; Pio, D.; Nunes, M.; Silvestre, A. Methodologies for bio-oil characterization from biomass pyrolysis: A review focused on GC-MS. *J. Anal. Appl. Pyrolysis* **2024**, *185*, 106850. [CrossRef]
6. Panić, S.; Đurišić-Mladenović, N.; Petronijević, M.; Stijepović, I.; Milanović, M.; Kozma, G.; Kukovecz, Á. Valorization of waste biomass towards biochar production—Characterization and perspectives for sustainable applications in Serbia. *Environ. Technol. Innov.* **2024**, *37*, 104043. [CrossRef]
7. Onokwai, A.O.; Ajisegiri, E.S.A.; Okokpujie, I.P.; Ibikunle, R.A.; Oki, M.; Dirisu, J.O. Characterization of lignocellulose biomass based on proximate, ultimate, structural composition, and thermal analysis. *Mater. Today Proc.* **2022**, *65*, 2156–2162. [CrossRef]
8. United States Energy Information Administration. Available online: https://www.eia.gov/energyexplained/biomass (accessed on 25 February 2026).
9. Singh, Y.D.; Mahanta, P.; Bora, U. Comprehensive characterization of lignocellulosic biomass through proximate, ultimate and compositional analysis for bioenergy production. *Renew. Energy* **2017**, *103*, 490–500. [CrossRef]
10. Hazman, N.; Isa, N.M.; Nasir, N.F.; Hussein, M.; Adebayo, D.S. The Proximate and Ultimate Composition of Pulverised Coconut Shell. *Int. J. Integr. Eng.* **2024**, *16*, 270–277. [CrossRef]
11. Zhang, Y.; Zhang, X.; Zhou, Z.; Liu, G.; Wang, C. A review of the conversion of wood biomass into high-performance bulk biochar: Pretreatment, modification, characterization, and wastewater application. *Sep. Purif. Technol.* **2025**, *361*, 131448. [CrossRef]
12. Manić, N.G.; Janković, B.; Stojiljković, D.D.; Jovanović, V.V.; Radojević, M.B. Tga-Dsc-Ms analysis of pyrolysis process of various agricultural residues. *Therm. Sci.* **2018**, *23*, 1457–1472. [CrossRef]
13. Maria del Pilar, N.E.; Villa, N.; Ceballos, F.; Chejne Janna, F. Characterization and valorization of oil palm biomass, derived materials, and applications. *Biomass Bioenergy* **2026**, *214*, 109472. [CrossRef]
14. Bahrami, A.; Soltani, N.; Pech-Canul, M.I.; Gutiérrez, C.A. Development of metal-matrix composites from industrial/agricultural waste materials and their derivatives. *Crit. Rev. Environ. Sci. Technol.* **2016**, *46*, 143–207. [CrossRef]
15. Awogbemi, O.; Adeleye, S.A.; Ojo, A.A. Experimental evaluation of proximate, ultimate, heating values, and structural composition of selected crop shells. *Discov. Sustain.* **2025**, *6*, 1093. [CrossRef]
16. Marrugo, G.; Valdés, C.F.; Chejne, F. Characterization of Colombian Agroindustrial Biomass Residues as Energy Resources. *Energy Fuels* **2016**, *30*, 8386–8398. [CrossRef]
17. Gani, A.; Adisalamun; Arkan D, M.R.; Suhendrayatna; Reza, M.; Erdiwansyah; Saiful; Desvita, H. Proximate and ultimate analysis of corncob biomass waste as raw material for biocoke fuel production. *Case Stud. Chem. Environ. Eng.* **2023**, *8*, 100525. [CrossRef]
18. Ghiasi, M.M.; Mohammadzadeh, O.; Zendehboudi, S.; Fgaier, H. Effective approach to assess higher heating value of biomass from ultimate and proximate analysis. *Can. J. Chem. Eng.* **2025**, *103*, 1155–1168. [CrossRef]
19. Nhuchhen, D.R.; Abdul Salam, P. Estimation of higher heating value of biomass from proximate analysis: A new approach. *Fuel* **2012**, *99*, 55–63. [CrossRef]
20. Friedl, A.; Padouvas, E.; Rotter, H.; Varmuza, K. Prediction of heating values of biomass fuel from elemental composition. *Anal. Chim. Acta* **2005**, *544*, 191–198. [CrossRef]
21. Park, S.; Kim, S.J.; Oh, K.C.; Cho, L.H.; Kim, D.H. Developing a Proximate Component Prediction Model of Biomass Based on Element Analysis. *Energies* **2023**, *16*, 509. [CrossRef]
22. Demirbas, A. Calculation of higher heating values of fatty acids. *Energy Sources Part A Recover. Util. Environ. Eff.* **2016**, *38*, 2693–2697. [CrossRef]

23. Huang, Y.F.; Lo, S.L. Predicting heating value of lignocellulosic biomass based on elemental analysis. *Energy* **2020**, *191*, 116501. [CrossRef]
24. Buckley, T.J. Calculation of higher heating values of biomass materials and waste components from elemental analyses. *Resour. Conserv. Recycl.* **1991**, *5*, 329–341. [CrossRef]
25. Annamalai, K.; Sweeten, J.M.; Ramalingam, S.C. Technical Notes: Estimation of Gross Heating Values of Biomass Fuels. *Trans. ASAE* **1987**, *30*, 1205–1208. [CrossRef]
26. Sheng, C.; Azevedo, J.L.T. Estimating the higher heating value of biomass fuels from basic analysis data. *Biomass Bioenergy* **2005**, *28*, 499–507. [CrossRef]
27. Channiwala, S.A.; Parikh, P.P. A unified correlation for estimating HHV of solid, liquid and gaseous fuels. *Fuel* **2002**, *81*, 1051–1063. [CrossRef]
28. Madakson, P.B.; Yawas, D.S.; Apasi, A. Characterization of Coconut Shell Ash for Potential Utilization in Metal Matrix Composites for Automotive Applications. *Int. J. Eng. Sci. Technol.* **2012**, *4*, 1190–1196.
29. Racero-Galaraga, D.; Rhenals-Julio, J.D.; Sofan-German, S.; Mendoza, J.M.; Bula-Silvera, A. Proximate analysis in biomass: Standards, applications and key characteristics. *Results Chem.* **2024**, *12*, 101886. [CrossRef]
30. Bianchini, L.; Colantoni, A.; Venanzi, R.; Cozzolino, L.; Picchio, R. Physicochemical Properties of Forest Wood Biomass for Bioenergy Application: A Review. *Forests* **2025**, *16*, 702. [CrossRef]
31. Shah, M.A.; Hayder, G.; Kumar, R.; Kumar, V.; Ahamad, T.; Kalam, A.; Soudagar, M.E.M.; Shamshuddin, S.Z.M.; Mubarak, N.M. Development of sustainable biomass residues for biofuels applications. *Sci. Rep.* **2023**, *13*, 14248. [CrossRef] [PubMed]
32. Ji, J.; Hu, X.; Zhang, X.; Zhang, Q.; Chen, L.; Zhuang, X.; Ma, L. Kinetic modeling of hydrothermal carbonization for lignocellulosic and protein-rich biomass: A multi-component reaction network approach. *Biomass Bioenergy* **2026**, *216*, 109676. [CrossRef]
33. Madhu, P.; Livingston, T.S.; Manickam, I.N. Fixed bed pyrolysis of lemongrass (Cymbopogon flexuosus): Bio-oil production and characterization. *Energy Sources Part A Recover. Util. Environ. Eff.* **2017**, *39*, 1359–1368. [CrossRef]
34. Morales-Máximo, M.; Gudiño-Macedo, R.; Rutiaga-Quiñones, J.G.; Coral-Huacuz, J.C.; Pintor-Ibarra, L.F.; López-Sosa, L.B.; Ruíz-García, V.M. Characterization of Residual Woody Biomass for the Production of Densified Solid Biofuels and Their Local Utilization. *Fuels* **2026**, *7*, 23. [CrossRef]
35. Yahya, A.M.; Adeleke, A.A.; Nzerem, P.; Ikubanni, P.P.; Ayuba, S.; Rasheed, H.A.; Gimba, A.; Okafor, I.; Okolie, J.A.; Paramasivam, P. Comprehensive Characterization of Some Selected Biomass for Bioenergy Production. *ACS Omega* **2023**, *8*, 43771–43791. [CrossRef] [PubMed]
36. Thomas, B.; Werner, K.; Ingwald, O.; Alexander, T. combustion properties of maize cobs-results from lab and pilot scale tests. In Proceedings of the 19th European Biomass Conference & Exhibition, Berlin, Germany, 6–10 June 2011; pp. 944–951.
37. Kpalo, S.Y.; Zainuddin, M.F. Briquettes from Agricultural Residues; An Alternative Clean and Sustainable Fuel for Domestic Cooking in Nasarawa State, Nigeria. *Energy Power* **2020**, *10*, 40–47. [CrossRef]
38. Platace, R.; Adamovics, A.; Poisa, L.; Cubars, E.; Bumane, S. Ash content in grass biomass yielded in 1st and 2nd cultivation year and evaluation of suitability thereof for pellet production. *Eng. Rural Dev.* **2015**, *14*, 541–545.
39. Olupot, P.W.; Candia, A.; Menya, E.; Walozi, R. Characterization of rice husk varieties in Uganda for biofuels and their techno-economic feasibility in gasification. *Chem. Eng. Res. Des.* **2016**, *107*, 63–72. [CrossRef]
40. Kumar, P.; Joshi, D.; Mathur, B. Sustainable development of AA6063 hybrid composites using agro-Waste and industrial waste reinforcements for enhanced wear resistance. *Can. Metall. Q.* **2026**, *4433*, 1–18. [CrossRef]
41. John, A.N.; Jike, N.B.N.; Nnakwo, K.C. Evaluation of microstructure, mechanical, and tribological behavior of agro-waste hybrid reinforced high-performance Al-Si-Mg metal matrix composites. *Next Mater.* **2026**, *11*, 101974. [CrossRef]
42. Williams, U.A.; Fayomi, O.S.I.; Ojediran, J.O. Sustainable reinforcement of aluminium 6063 with plantain peel ash: Microstructural, mechanical, and corrosion performance. *Next Mater.* **2025**, *9*, 100986. [CrossRef]
43. Yusuf, A.A.; Inambao, F.L. Characterization of Ugandan biomass wastes as the potential candidates towards bioenergy production. *Renew. Sustain. Energy Rev.* **2019**, *117*, 109477. [CrossRef]
44. Uzoagba, C.E.J.; Okoroigwe, E.; Kadivar, M.; Anye, V.C.; Bello, A.; Ezealigo, U.; Ngasoh, F.O.; Pereira, H.; Onwualu, P.A. Characterization of Wood, Leaves, Barks, and pod wastes from Prosopis africana biomass for biofuel production. *Waste Manag. Bull.* **2024**, *2*, 172–182. [CrossRef]
45. Varma, A.K.; Singh, S.; Rathore, A.K.; Thakur, L.S.; Shankar, R.; Mondal, P. Investigation of kinetic and thermodynamic parameters for pyrolysis of peanut shell using thermogravimetric analysis. *Biomass Convers. Biorefin.* **2022**, *12*, 4877–4888. [CrossRef]
46. Rambhatla, N.; Panicker, T.F.; Mishra, R.K.; Manjeshwar, S.K.; Sharma, A. Biomass pyrolysis for biochar production: Study of kinetics parameters and effect of temperature on biochar yield and its physicochemical properties. *Results Eng.* **2024**, *25*, 103679. [CrossRef]
47. Suhas; Chaudhary, M.; Chaudhary, S.; Chaubey, S.; Cansado, I.P.d.P.; Dehghani, M.H.; Tyagi, I.; Gaur, R. Transforming Biomass Waste into Hydrochars and Porous Activated Carbon: A Characterization Study. *Resources* **2025**, *14*, 34. [CrossRef]

48. Mary Onyelucheya, C.; Tagbo Nwabanne, J.; Olawale Daramola, M.; Ayodele Iwarere, S. Chemical, Thermogravimetric and Elemental Characterization of Nigerian Groundnut and Cowpea Shells for Sustainable Valorization. *IOP Conf. Ser. Earth Environ. Sci.* **2024**, *1322*, 012003. [CrossRef]
49. El-Sayed, S.A.; Khass, T.M.; Mostafa, M.E. Thermal degradation behaviour and chemical kinetic characteristics of biomass pyrolysis using TG/DTG/DTA techniques. *Biomass Convers. Biorefin.* **2024**, *14*, 17779–17803. [CrossRef]
50. Volpe, M.; Picone, A.; Bellardita, M.; Messineo, A. Hydrothermal carbonization and photocatalytic reforming as a two-step combined strategy for the complete valorization of citrus waste. *Biomass Bioenergy* **2026**, *216*, 109707. [CrossRef]
51. Durai, P.N.; Arunprasath, K.; Divakaran, D.; Kumar, R.; Senthamaraikannan, P.; Suyambulingam, I.; Viswalingam, K. Exploring agro waste as a sustainable reinforcement in biopolymer composites–a review. *Green Chem. Lett. Rev.* **2025**, *18*, 2589532. [CrossRef]
52. Nandiyanto, A.B.D.; Oktiani, R.; Ragadhita, R. How to read and interpret ftir spectroscope of organic material. *Indones. J. Sci. Technol.* **2019**, *4*, 97–118. [CrossRef]
53. Cruz, N.C.; Silva, F.C.; Tarelho, L.A.C.; Rodrigues, S.M. Critical review of key variables affecting potential recycling applications of ash produced at large-scale biomass combustion plants. *Resour. Conserv. Recycl.* **2019**, *150*, 104427. [CrossRef]
54. Tan, Z.; Lagerkvist, A. Phosphorus recovery from the biomass ash: A review. *Renew. Sustain. Energy Rev.* **2011**, *15*, 3588–3602. [CrossRef]
55. Dwivedi, S.P.; Dwivedi, V.K.; Yadav, R. Tribological and Corrosion Behavior of Eggshell and Agro-waste RHA Reinforced Al Alloy Composite Material with and without Ball-Milling. *J. Inst. Eng. Ser. D* **2023**, *105*, 449–460. [CrossRef]
56. Niu, Y.; Tan, H.; Hui, S. Ash-related issues during biomass combustion: Alkali-induced slagging, silicate melt-induced slagging (ash fusion), agglomeration, corrosion, ash utilization, and related countermeasures. *Prog. Energy Combust. Sci.* **2016**, *52*, 1–61. [CrossRef]
57. Abshalomu, Y.; Jyothi, Y.; Balamurugan, K.; Selvaraj, R. Effect of Varied Cashew Nut Ash Reinforcement in Aluminum Matrix Composite. *Adv. Mater. Sci. Eng.* **2023**, *2023*, 3383777. [CrossRef]
58. Erdiwansyah; Gani, A.; Desvita, H.; Mahidin; Viena, V.; Mamat, R.; Sardjono, R.E. Analysis study and experiments SEM-EDS of particles and porosity of empty fruit bunches. *Case Stud. Chem. Environ. Eng.* **2024**, *9*, 100773. [CrossRef]

Disclaimer/Publisher's Note: The statements, opinions and data contained in all publications are solely those of the individual author(s) and contributor(s) and not of MDPI and/or the editor(s). MDPI and/or the editor(s) disclaim responsibility for any injury to people or property resulting from any ideas, methods, instructions or products referred to in the content.